

# ULTRASONIC MEASUREMENTS IN ICE SLURRY GENERATION BY DIRECT CONTACT EVAPORATION

Didier Vuarnoz\*, D. Ata-Caesar\*, Osmann Sari\*, Peter William Egolf\*

\*EIVD, Route de Cheseaux 1, CH-1401 Yverdon-les-Bains, [dvuarnoz@eivd.ch](mailto:dvuarnoz@eivd.ch)

## ABSTRACT

Important reductions of refrigerant amounts can be achieved by using secondary refrigeration fluids. Ice slurry is a two-phase fluid and thus, compared to single phase secondary refrigeration fluids, offers the advantage of the latent heat of fusion when the ice phase melts during heat exchange. Therefore, the challenges that the introduction of ice slurry as a common thermal fluid is facing are, in the first place, how to generate ice slurry in an efficient and ecological way. Optimal design of a direct contact ice slurry generator requires studying the injection and the mechanisms of the evaporation of the refrigerant in the aqueous solution. The evaporation chamber is the main domain of our investigations presented in this paper. Some aspects of the evolution of the liquid-to-gas phase-change of the refrigerant, and of the liquid to solid phase-change of the water are presented in this article. Basic theory, velocity profiles achieved by Ultrasonic Doppler Method (UDM), and extracted values from measurements help to understand how to optimise the process of ice creation by an expanding jet of refrigerant in a column of water.

**Keywords:** Ice-slurry, jet, bubbles, drop, drobble, refrigerant.

## INTRODUCTION

Ice slurry consists of numerous ice particles with an average size below 1mm, suspended in a carrier fluid. It is therefore a two-phase colloidal suspension, classed in the family of the Phase Change Slurries PCS. There are two main different methods of producing ice slurry: the heterogeneous nucleation and the homogeneous nucleation. In this paper we deal only with the *homogeneous nucleation*. *Direct injection*, where the non-miscible refrigerant (dispersed phase) is injected into the brine fluid (continuous phase), is an interesting method in terms of energy and cost efficiency. (Chuard & Fortuin, 1999) with C4F8, (Wobst and Vollmer, 1999) with R600a and (K. Kiatsiriroat *et al.*, 2003) produced ice slurry using this type of generator.

In most research approaches, the first approximation to study direct contact evaporation is based on the study of single drops evaporating in an immiscible medium. A detailed review of the state of the art was performed by (Lugo, 2004). It has been confirmed experimentally, that the configuration of a single drop during evaporation is that given in (Sideman & Taitel, 1964). As soon as the drop starts to evaporate, the liquid forms a meniscus at the bottom of the vapour bubble which begins to rise. Trajectories of rising bubbles were studied by (Zun, 1986), (Tomiyama *et al.*, 1993) and (Sletta *et al.*, 04). Theoretical and experimental single drop studies have been carried out by many authors. (Sideman & Taitel 1964) used the general drop-bubble configuration to solve the energy equation; they give an expression of the average Nusselt number (Nu) as a function of the Peclet number (Pe) and the opening angle  $\beta$  (fig. 2); they assume that heat transfer only takes place at the liquid-liquid interface of the evaporating drop.

They validate their expressions with experimental results obtained with pentane and butane drops injected into distilled or sea water. (Tochitani *et al.*, 1977) studied the evaporation of single drops of pentane and furan in aqueous glycerol. The same authors compare the experimental heat transfer characteristics with a Stokes flow model. Heat transfer coefficients are determined using the liquid-liquid interfacial area or the total surface area of the evaporating drop as the heat exchange surface. (Shimizu et Mori, 1988) dealt with the evaporation of single drops of R113 and n-pentane injected into water under pressures up to 0.48 MPa. The heat flow rate is determined from the volume variation; the authors propose two configurations: 1) the drop consists of saturated liquid and saturated vapour of the dispersed phase (explanation given in the remainder); and 2) the drop consists of saturated liquid of dispersed phase and saturated vapours of both the water and the dispersed phase.

The main objective of this study is, to investigate if Ultrasonic Doppler measurements are adequate to better understand the interrelated phenomena involved in such injection and evaporation of the refrigerant including the ice creation. (Ata-Caesar, 2004) performed a complete study on the choice of the refrigerant for this ice generation technology. For laboratory safety reasons however, the present studies were done with the refrigerant C<sub>4</sub>F<sub>8</sub>.

## BASIC THEORY

### The injection

The configuration of the injected refrigerant can be classified into the four flow regimes shown in fig. 1 (Clift *et al.* 1978). With interfacial tension as a parameter, the regimes are a function of the nozzle characteristics and the flow rate of the

injected fluid. Based on the following definition of the injection Reynolds number as proposed in (1):

$$Re_{inj} = \delta_c * D_{inj} * U_{inj} / \mu_c \quad (1)$$

(Meister and Scheele, 1969) point out three flow regimes. For  $Re_{inj}$  below 300 the regime is drop to drop. For  $Re_{inj}$  between 300 and 3000 the injected fluid configures in a column-like flow pattern. The last case is the turbulent regime, often denoted atomization. We have investigated the drop to drop regime.

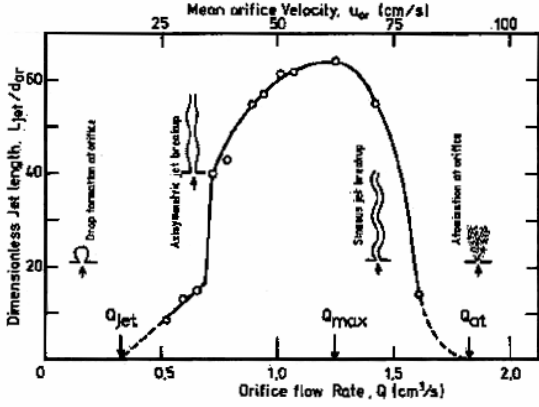


Fig. 1: Injection regime as a function of the mass flow and the nozzle characteristics.

### The evaporation

To schematize the evolution of the evaporating drop, a simplified model was used (Lugo, 2004) to describe the geometry of the evaporating refrigerant drop (fig 2). The word “drobble” in the following text refers to a liquid drop during evaporation.

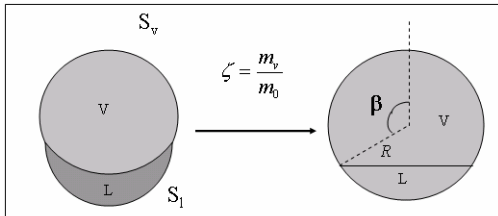


Fig. 2: Geometrical description of a drop during evaporation. The drop quality ( $\zeta$ ) is the ratio of the vapour to initial drop mass.

The radius as a function of drobble quality is expressed by:

$$R^3 = R_0^3 \left[ 1 + \zeta \left( \frac{\rho_l}{\rho_v} - 1 \right) \right] \quad (2)$$

The bubble opening angle as a function of drobble quality is expressed by:

$$3 \cos \beta - \cos^3 \beta + 2 = \frac{4(1 - \zeta)}{1 + \zeta \left( \frac{\rho_l}{\rho_v} - 1 \right)} \quad (3)$$

where  $\beta$  is the opening angle,  $R$  and  $R_0$  are the radius and the initial radius,  $\rho_l$  and  $\rho_v$  are refrigerant liquid and vapour densities. These equations can be used to predict the growth of the drobble. The drobble velocity  $U$  is obtained by simplifying and solving the following momentum equation:

$$\rho_d V_d U \frac{dU}{dz} = (\rho_c - \rho_d) \frac{4}{3} \pi R^3 g - \frac{\pi}{2} \rho_c C_D R^2 U^2 \quad (4)$$

where  $g$  is the gravity,  $V$  is the volume,  $C_D$  is the drag coefficient,  $\rho_c$  is the carrier fluid density,  $z$  is the vertical coordinate and index  $d$  stands for “dispersed phase” (related to the system drop + bubble). Rigorously, other terms should appear in this equation (added mass, parachute effect, etc.) but they prove to be negligible as the evaporation starts. The motion is mainly controlled by buoyancy and drag forces. There are many expressions for the drag coefficient of drops and bubbles, but many authors use only some formulae for air bubbles. Heat transfer is governed by:

$$\dot{Q} = S_{hex} h (T_c - T_d) = U \rho_d V_d \Delta h_v \frac{d\zeta}{dz} \quad (5)$$

where  $\dot{Q}$  is the heat exchanged between the carrier fluid and the particle per unit time,  $S_{hex}$  and  $h$  are the heat transfer surface and the heat transfer coefficient (they vary widely from one author to another),  $T_c$  and  $T_d$  are the temperature of the carrier fluid and the particle temperatures (for the evaporation of a single drop, both are assumed to be constant) and  $\Delta h_v$  is the enthalpy of vaporization of the refrigerant.

## EXPERIMENTAL METHOD

### The experimental setup

Our experimental setup for ice slurry generation (fig. 3) is identical to the one of (Chuard & Fortuin 1999).

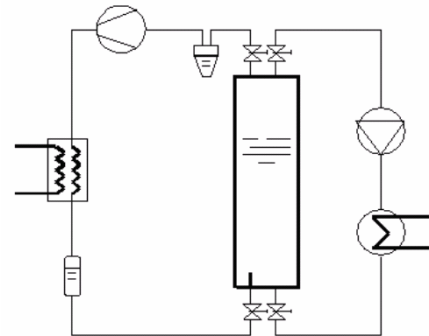


Fig. 3: Schematic drawing of the direct injection system.

In this vapour compression cycle direct contact evaporation is applied. Technical differences from the conventional installations are the evaporation chamber and the injection of refrigerant. The injection is performed through a nozzle, which causes not only the expansion of the refrigerant but also the movement and turbulence of the mixture in the evaporation chamber. A tube in Plexiglas of 400mm diameter was fixed 3 cm above the nozzle to concentrate the injected flux of refrigerant. The refrigerant expands and evaporates inside the evaporation chamber at constant pressure and constant temperature ( $<0^\circ\text{C}$ ). The vapour rises through the contents of the chamber and the compressor sucks it away. During the evaporation, the latent heat of vaporization is withdrawn from the surrounding carrier fluid. At locations where this cooling effect leads to temperatures slightly below the freezing temperature of the aqueous solution, the water in the solution begins to freeze to tiny ice particles, which are suspended in the remaining unfrozen aqueous solution. This way, a certain amount of the water of the solution can be transformed to finely dispersed ice. The remaining aqueous solution has a

higher concentration of freezing depressing agent and stays liquid.

The applied measurement device for experimentally studying the injection is an Ultrasonic Velocity Profiler UVP-XW3. The positions of the UVP probes are detailed in fig. 4. The UVP measurements were performed separately for each height.

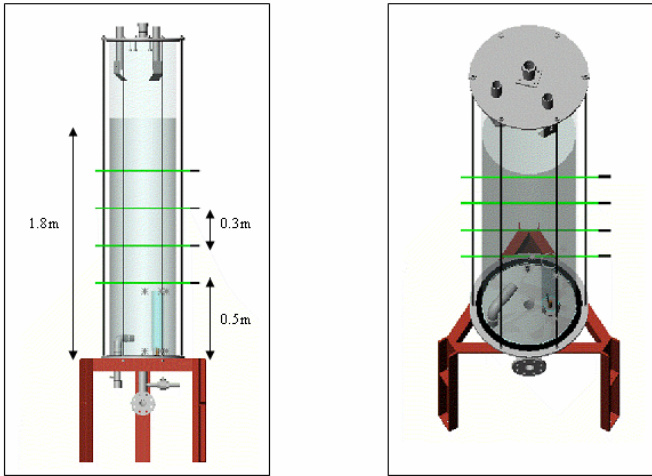


Fig. 4: Drawing of the evaporation chamber with the position of the four ultrasonic transducers of 2 MHz.

## RESULTS AND DISCUSSION

One way to show the results of a UVP measurement is the colour plot showed in fig. 5. From this plot, the diameter, velocity and horizontal position of drobbles can be extracted. Table 1 shows average values determined from recorded data such as in fig. 5 and fig. 6. The velocity, size and drobble position along the ultrasonic beam are listed for the four heights where measurements were taken.

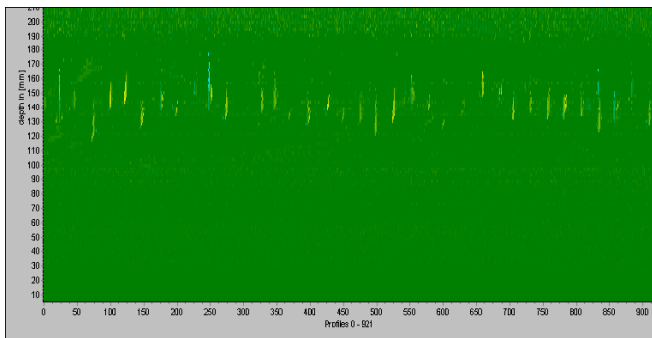


Fig. 5: UDM series of thousand velocity profile measurements of drop to drop injection regime at  $z = 800\text{mm}$  above the injection nozzle.

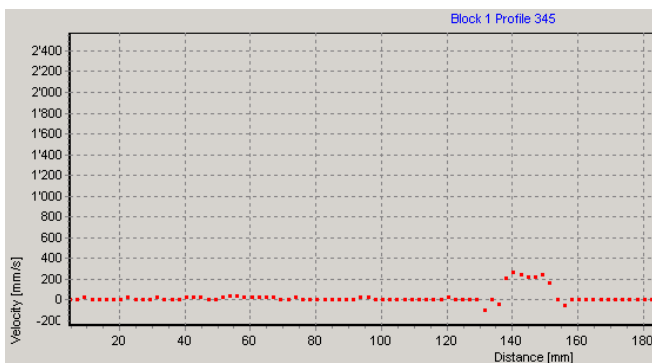


Fig 6: Velocity profile used for the determination of the diameter and velocity of the drobbles at  $z = 800\text{mm}$ .

Level	Z [m]	D [mm]	U [m/s]	$x_{\max}$ [mm]	$f_{\text{ini}}$ [Hz]
1	0.5	22.2	0.366	-3.9 / 4.5	0.737
2	0.8	26.6	0.432	-12.4 / 10.8	3.119
3	1.1	23.7	0.448	-17.4 / 16.1	0.758
4	1.4	24.9	0.397	-21.6 / 18.7	1.4

Table 1: Synthesis of mean values determined from data of Ultrasonic Doppler Method investigation.

The probability that the trajectory of a drobble crosses the ultrasonic beam (diameter =  $X$  mm) decreases with the distance between the nozzle and the investigated position. The drobble diameter for each level is determined from the maximal trace of each measurement series. Figure 7 shows the drobble diameter versus column height determined with UVP (points). The measured value at the second level deviates rather strongly though. The dashed line indicates the rapid drobble growth shortly after injection of the liquid drop.

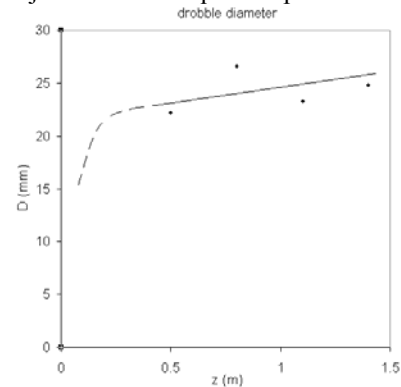


Fig. 7: Experimental results of the drobble diameter versus the distance  $z$ .

Figure 8 shows the drop velocity as a function of the column height determined with UVP (points). The tendency is shown with the line. The measured value at the highest level deviates rather strongly though. The dashed line indicates the strong drobble acceleration due to its rapid growth shortly after injection of the liquid drop.

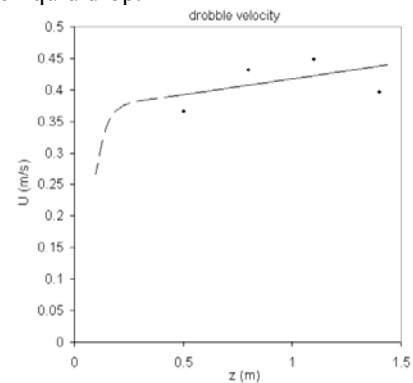


Fig. 8: Experimental results of the drop velocity versus the distance  $z$ .

A two dimensional description of the drobble trajectory can be determined by looking at the position of each particle appearing in the measured velocity profile series (as in fig. 6). For each investigated level, the two particles found at the largest opposing distances from the nozzle axis are represented in figure 9.

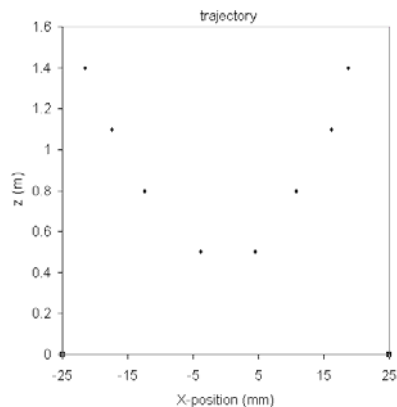


Fig. 9: Maximal lateral position versus column height  $z$  obtained UVP. The axis of the nozzle is located at  $X = 0$ .

Ultrasonic Doppler measurements appear to be suitable for investigating the fluid dynamic behaviour of refrigerant drops evaporating in a non-miscible fluid as occurs in the evaporation chamber of a direct contact ice slurry generator. Comparison of the UDM experimental results with numerical simulations of the aforementioned fluid dynamic behaviour can provide an efficient approach towards utilising UDM in experimental multiphase fluid dynamics investigations. At present, commercial Computational Fluid Dynamic (CFD) codes can be efficiently applied to investigate bubbly flows, drag on particles and the influence of turbulence on flow patterns. However, the phenomena occurring during the evaporation of liquid drops in a liquid surrounding are not yet implemented in commercial CFD codes. This limitation calls for specialized numerical simulation codes, which take the drop to bubble phase change into account, in order to be able to compare theoretical to experimental results for the entire drop to bubble evolution. Numerical investigations (Lugo, 2004) have shown remarkable dependence of the drobble behaviour on the initial conditions of the injected refrigerant drop, such as the initial diameter and velocity. These necessary parameters for reasonable theoretical investigations are although difficult to determine.

## CONCLUSIONS AND OUTLOOK

The Ultrasonic Doppler Method has been applied to the process of ice slurry generation by direct injection of a refrigerant into an aqueous solution. Some theory of the physics involved, such as the injection regime and the evaporation processes, has been shown. The main objective of this work has been to investigate the fluid dynamic behaviour of evaporating refrigerant drops in an immiscible fluid and the approach taken has been to evaluate how suitable the UDM technique is for such investigations.

The diameter, the velocity and the position of evaporating refrigerant drops were determined from the results of Ultrasonic Doppler measurements. The determined values agree well with numerical results. For better comparison with numerical simulation, improved studies of the initial conditions of the injected refrigerant drop are needed.

## ACKNOWLEDGEMENT

The authors are especially grateful to R. Lugo for the active collaboration during his PhD work on a six months stay in Yverdon-les-Bains. The "Haute Ecole Spécialisée de Suisse Occidentale (HES-SO)" is gratefully acknowledged.

## REFERENCES

1. Chuard M., Fortuin J., 1999, COLDECO – A new technology system for production and storage of ice. *Proceedings of the First Workshop on Ice Slurries*. IIF/IIR : 140-146.
2. Wobs E., Vollmer D., 1999, Ice slurry generation by direct evaporating of refrigerant. In: *Proceedings of the First Workshop on Ice Slurries*. IIF/IIR : 126-132.
3. Kiatsisriroat T., Vithayasai S., Vorayos N., Nuntaphan A., Vorayos N., 2003, Heat transfer prediction for a direct contact ice thermal energy storage. *Energy Conversion Management* 44 : 497-508.
4. Lugo, R., 2004, Contribution à l'étude de deux méthodes de fabrication de coulis de glace par contact direct: Evaporation sous vide et injection directe. Thèse du Conservatoire National des Arts et Métiers.
5. Sideman S., Taitel Y., 1964, Direct-contact heat transfer with change of phase: evaporation of drops in an immiscible liquid medium. *Int. J. Heat Mass Transfer* 7: 1273-1289.
6. Zun, I., 1986, The non-rectilinear motion of bubbles rising through a stagnant and disturbed liquid. *Proc. World Cong. III of Chem. Eng.*, vol II. 214-217.
7. J. Sletta, D. Vuarnoz, O. Sari, D. Ata-Caesar, P.W. Egolf, , 2004, Production de « coulis de glace » à germination spontanée : Système COLDECO®, Rapport Scientifique Final HES-SO.
8. Tomiyama A., Zun I., Sou A., Sakaguchi T., 1993, Numerical analysis of bubble motion with the VOF method. *Nucl. Eng. Des.* 141: 69-82.
9. Tochitani Y., Nagagawa T., Mori Y., Komotori K., 1977, Vaporization of single liquid drops in a immiscible liquid. Part II: Heat transfer characteristics. *Wärme-und Stoffübertragung*. 10:71-79.
10. Shimizu Y., Mori Y. Evaporation of single drops in an immiscible liquid at elevated pressure. Experimental study with n-pentane and R113 drops in water. *Int. J. Heat Mass Transfer* 31:1843-1851.
11. Ata-Caesar, D., Sletta, J., Sari, O., Egolf, P.W., 2004, Refrigerant choice for ice-slurry production in direct contact heat exchangers, *Proc. of the Sixth Gustav Lorentzen Conference on Natural Working Fluids of the International Institute of Refrigeration*, Glasgow, 29<sup>th</sup> of Aug. – 1<sup>st</sup> of Sept. 2004.

## NOMENCLATURE

### Latin symbols

$C_D$	drag coefficient
$D$	mean diameter (m)
$g$	gravity ( $\text{m s}^{-2}$ )
$h$	heat transfer coefficient ( $\text{W m}^{-2} \text{K}^{-1}$ )
$\Delta h_v$	enthalpy of vaporization ( $\text{kJ kg}^{-1}$ )
$\dot{Q}$	power (W)
$R$	radius (m)
$S_{hex}$	heat exchange surface ( $\text{m}^2$ )
$T$	temperature ( $^{\circ}\text{C}$ )
$U$	velocity ( $\text{m s}^{-1}$ )
$V$	volume ( $\text{m}^3$ )
$z$	vertical coordinate (m)

### Greek symbols

$\beta$	opening angle
$\rho$	density ( $\text{kg/m}^3$ )
$\zeta$	drop quality
$\mu$	dynamic viscosity ( $\text{Pa s}$ )

### Subscripts

$c$	continuous phase
$d$	dispersed phase
$l$	dispersed liquid phase
$v$	dispersed vapour phase
inj	injection